

## ROLE OF FLAMEFRONT MOTION AND CRITERION FOR GLOBAL QUASI-STEADINESS IN DROPLET BURNING

LONGTING HE, STEPHEN D. TSE, AND CHUNG K. LAW

*Department of Mechanical and Aerospace Engineering  
Princeton University  
Princeton, NJ 08544, USA*

A theoretical study has been conducted on the role of the flamefront motion in droplet burning to determine the range of validity of the classical quasi-steady theory in predicting the flame standoff ratio, as well as its implication on transient fuel vapor accumulation/depletion. Recognizing that flamefront motion can be induced by droplet surface regression, by initial conditions, and by far-field unsteadiness, and that the flamefront standoff ratio is in general large, of the order of 10, it is phenomenologically anticipated that small flamefront velocities can lead to large variations of the mass flow rate. Furthermore, it is demonstrated that the influence of this flamefront motion can be characterized by a quasi-steady parameter  $Q_s$ , which is the product of the cube of the standoff ratio and the ratio of the gas to liquid densities, such that the influence is large when it is  $O(1)$ , and small otherwise. By working in the flame coordinate and, hence, naturally allowing for this motion, and by further assuming gas-phase quasi-steadiness (in this coordinate), calculated results show that the standoff ratio continuously increases with time for  $O(1)$  values of  $Q_s$  but approaches a constant, which is close to but exceeds the  $d^2$ -law prediction, when it is sufficiently small. The present generalized transient formulation also provides a rigorous description of fuel vapor accumulation effects related to the initial condition, demonstrates that these effects can indeed be accounted for on the basis of gas-phase quasi-steadiness, and allows for the simultaneous inclusion of far-field transient diffusion effects.

### Introduction

The basic droplet combustion model was formulated in the 1950s by Godsave [1], Spalding [2], Goldsmith and Penner [3], and Williams [4] for an isolated, single-component, constant-temperature, droplet burning in a stagnant, oxidizing environment. Since the ratio of the gas density  $\bar{\rho}$  to liquid density  $\bar{\rho}_l$ ,  $\varepsilon = \bar{\rho}/\bar{\rho}_l$  is much smaller than unity for applications not close to the thermodynamic critical state [4], the gas diffusion time based on the droplet size is much smaller than the droplet lifetime. As a result, unsteady effects related to the regression of the droplet surface can be neglected. This leads to the classical quasi-steady (CQS) approximation for droplet combustion, termed the  $d^2$ -law, which is characterized by the following features: (1) The square of the droplet diameter decreases linearly with time; (2) the flamefront standoff ratio, defined as the ratio of the flame radius  $\tilde{r}_f$  to the droplet radius  $\tilde{r}_s$ ,  $\kappa_{CQS} \equiv \tilde{r}_f/\tilde{r}_s$ , is constant; (3) the flame temperature is constant; and (4) flame burnout is coincident with complete droplet consumption. Experiments have repeatedly shown that (1) largely holds, subsequent to a brief, initial period of droplet heating [1–3,5,6]. However, it has also been observed that the standoff ratio and temperature of the flame may not be constant [5,6], implying failure of the classical

$d^2$ -law to describe the cumulative heat release. A number of studies have been subsequently carried out that attribute these phenomena to various effects of unsteadiness, which are not considered in the classical theory. Reviews on droplet combustion can be found in the literature [7,8].

To explain the discrepancy related to the flame standoff ratio, Waldman [9] and Crespo and Liñán [10] analyzed the far-field transient diffusion effect. It was suggested that since the gas velocity is inversely proportional to the square of the droplet radius, in a distance  $\tilde{r}$  far from the droplet surface ( $\tilde{r}/\tilde{r}_s > 1/\varepsilon^{1/2} \gg 1$ ), the local Péclet number becomes  $O(\varepsilon)$  and is therefore very small. The problem is then described by an unsteady diffusive process, with the inner field specified by fuel consumption rate at the flame being equal to the fuel evaporation rate at the droplet surface, as in the CQS approximation; and the far-field unsteady effect was taken into account via multiscale matching [9,10]. It was shown that the far-field unsteady effect induced by the droplet surface regression contributes a correction of the order of  $O(\varepsilon^{1/2})$  to the CQS solution.

Law et al. [6] and Botros et al. [11] subsequently showed that unsteadiness can also be caused by initial conditions. Specifically, since a flame is initially situated very close to the droplet surface upon ignition, the fuel mass consumption rate at the flame

is smaller than the fuel evaporation rate at the droplet surface. Furthermore, due to volume effects, the amount of fuel vapor in the inner region to the flame can be substantial, with accumulation of fuel mass causing the outward spreading of the reaction front after ignition.

In the gas-phase analyses of the CQS theory and the far-field unsteady diffusion theory of Waldman [9] and Crespo and Liñán [10], it is assumed that the droplet surface regression velocity, nondimensionalized by the gas velocity at the surface,  $U_s = (d\tilde{r}_s/d\tilde{t})/\tilde{u}_s$ , is respectively zero and  $O(\varepsilon)$ , and that the mass flow rate across the reaction front,  $\tilde{m}_f$ , is always the same as that at the droplet surface,  $\tilde{m}_s$ . Implicit in such derivations is also the assumption that the nondimensional flamefront velocity,  $U_f \equiv (d\tilde{r}_f/d\tilde{t})/\tilde{u}_s$ , is at most  $O(\varepsilon)$ . However, as can be seen from feature (2) of the classical theory, in order for the standoff ratio  $\kappa$  to remain constant, the flame must spread with a nondimensional velocity,  $U_f \equiv (d\tilde{r}_f/d\tilde{t})/\tilde{u}_s = \kappa_{CQS} (d\tilde{r}_s/d\tilde{t})/\tilde{u}_s$ . Since the CQS theory predicts values of  $\kappa_{CQS}$  of up to 40 for hydrocarbon droplets burning in air,  $U_f$  can actually assume values substantially larger than  $O(\varepsilon)$ . Consequently, by not explicitly considering the motion of the flamefront in the derivations, previous theories are not self-consistent and, indeed, violate mass conservation.

The present work rigorously develops the droplet combustion model by properly maintaining mass conservation, thereby shoring a physically sound base on top of which unsteady effects such as far-field diffusion and fuel vapor accumulations can then be added and appropriately investigated. By placing the initial position of the flame at the CQS value and neglecting far-field effects, the present work examines the unsteady effect due to a regressing droplet surface by explicitly treating the role of flamefront motion. As a consequence, a new criterion is deduced that specifies situations under which the instantaneous motion of the flamefront is indeed  $O(\varepsilon)$  and thus negligible, thereby indicating when the  $d^2$ -law is adequate in describing the flamefront position.

In the following we sequentially present the analysis and criterion for global quasi-steadiness, formulation of the problem, including the quasi-steady model that takes into account the flamefront motion, and calculated results demonstrating the dependence of the dynamics of the flamefront motion on the various system parameters.

### Physical Analysis and Criterion

To begin with, let us investigate why and when the motion of the reaction front is important. Considering that the ratio of the volume enclosed by the flamefront to that of the droplet is  $\kappa_{CQS}^3$ , a droplet-surface regression rate of  $(d\tilde{r}_s/d\tilde{t}) = \varepsilon\tilde{u}_s$  produces a total mass flow rate variation of the order of  $\varepsilon\kappa_{CQS}^3$

between the droplet surface and the reaction front. Thus the motion of the reaction front becomes important when

$$\varepsilon\kappa_{CQS}^3 = O(1) \text{ or } \varepsilon\kappa_{CQS}^3 \gg 1 \quad (1a)$$

and can be neglected when

$$\varepsilon\kappa_{CQS}^3 \ll 1 \quad (1b)$$

In arriving at the preceding criterion, we have made the nonessential assumption that the density ratio for the gas mixtures between the droplet surface and the reaction front is  $O(1)$ . We therefore define  $Q_s \equiv \varepsilon\kappa_{CQS}^3$  as a nondimensional quasi-steady parameter. Since  $\kappa > 1$ , the classical theory can be applied when  $\varepsilon \ll 1$  and  $\kappa = O(1)$ . Thus, the effect related to the motion of the reaction front becomes important for  $\kappa_{CQS} \sim \varepsilon^{-1/3}$  or larger. For hydrocarbon droplet combustion in atmospheric air,  $\varepsilon \sim (10^{-3} \text{ to } 10^{-2})$ , and the experimental standoff ratio  $\kappa_{CQS}$  typically varies from 5 to 20. The mass flow rate variation,  $Q_s$ , is therefore of the order of  $10^{-1}$  to  $10^2$ , indicating that the motion of the reaction front is, in general, important even if the combustion started out with the flame situated at the quasi-steady value such that the fuel vapor accumulation effect due to initial conditions is minimized. These transient effects due to the flamefront motion are further aggravated for droplets burning in either asphyxiated or supercritical environments for which  $\kappa \gg 1$  and  $\varepsilon = O(1)$ , respectively [6,12].

The criterion given in equations 1a and 1b can be easily understood in that  $Q_s$  corresponds approximately to the ratio of the total mass of the fuel vapor to the mass of the droplet. The motion of the flamefront becomes crucial when the total mass of the fuel vapor is of the order of that within the droplet. The CQS theory is therefore adequate only when the total mass of the fuel vapor enclosed by the reaction front is much smaller than that of the droplet. The importance of the motion of the flamefront is also exhibited when the initial conditions are different from the CQS solutions. For example, if after ignition the reaction front is initially situated at a position closer to the droplet surface than that predicted by the classical theory, as mentioned earlier, the evaporation rate at the droplet surface would be larger than the consumption rate at the reaction front. Such an event results in fuel vapor accumulation between the droplet surface and the flame, causing the flame to move away from the surface [6]. Similar arguments then reveal that this mass accumulation effect is important when  $\varepsilon\kappa^3 = O(1)$  or  $\varepsilon\kappa^3 \gg 1$ .

We note in passing that from consideration of the far-field transient diffusion effect, Williams [13] deduced that when

$$\varepsilon\kappa_{CQS}^3 \left[ 8 \ln(1 + \alpha_{0,\infty}) \frac{\tilde{r}_s^2}{\tilde{r}_{s,0}^2} \right] > 1 \quad (2)$$

CQS theory cannot describe the flamefront position. Clearly, when the group of parameters within the square brackets of criterion (2) is  $O(1)$ , Williams's criterion is similar to ours obtained by considering the role of flamefront motion. However, at the late stage of droplet burning, when the droplet radius becomes much smaller than its initial radius,  $\tilde{r}_s \ll \tilde{r}_{s,0}$ , criterion (2) suggests that droplet burning will always be describable by the CQS theory which is different from the present reasoning.

### Formulation

To quantify the importance of the motion of the flamefront, we consider an isolated, single-component, droplet burning in a stagnant, oxidizing environment. For simplicity, we assume an infinitely fast, one-step overall reaction and constant values of the molecular weight, specific heat  $\tilde{c}_p$ , thermal conductivity  $\tilde{\lambda}$ , and density-weighted diffusivity  $\tilde{\rho}\tilde{D}$ . Variables overscripted with “ $\sim$ ” are dimensional. The mass, energy, and species conservation equations, in a reference frame moving with the reaction front, are

$$\tilde{r}^2 \frac{\partial \tilde{\rho}}{\partial \tilde{t}} + \frac{\partial \tilde{m}}{\partial \tilde{x}} + 2\tilde{r}\tilde{\rho}\tilde{U}_f = 0 \quad (3a)$$

$$\begin{aligned} \tilde{\rho}\tilde{r}^2 \frac{\partial \tilde{T}}{\partial \tilde{t}} + \tilde{m} \frac{\partial \tilde{T}}{\partial \tilde{x}} &= \frac{1}{\tilde{c}_p} \frac{\partial}{\partial \tilde{x}} \left( \tilde{r}^2 \tilde{\lambda} \frac{\partial \tilde{T}}{\partial \tilde{x}} \right) \\ &+ \frac{\tilde{\rho}\tilde{Q}}{\tilde{c}_p} \tilde{r}^2 \tilde{\omega} \end{aligned} \quad (3b)$$

$$\begin{aligned} \tilde{\rho}\tilde{r}^2 \frac{\partial \tilde{Y}_F}{\partial \tilde{t}} + \tilde{m} \frac{\partial \tilde{Y}_F}{\partial \tilde{x}} &= \frac{\partial}{\partial \tilde{x}} \left( \tilde{r}^2 \tilde{\rho}\tilde{D} \frac{\partial \tilde{Y}_F}{\partial \tilde{x}} \right) \\ &- \tilde{r}^2 \tilde{\rho}\tilde{\omega} \end{aligned} \quad (3c)$$

$$\begin{aligned} \tilde{\rho}\tilde{r}^2 \frac{\partial \tilde{Y}_O}{\partial \tilde{t}} + \tilde{m} \frac{\partial \tilde{Y}_O}{\partial \tilde{x}} &= \frac{\partial}{\partial \tilde{x}} \left( \tilde{r}^2 \tilde{\rho}\tilde{D} \frac{\partial \tilde{Y}_O}{\partial \tilde{x}} \right) \\ &- \tilde{r}^2 \nu_O W_O \tilde{\rho}\tilde{\omega} \end{aligned} \quad (3d)$$

where

$$\tilde{m} \equiv \tilde{\rho}(\tilde{u} - \tilde{U}_f)\tilde{r}^2, \quad d\tilde{x} \equiv d\tilde{r} - \tilde{U}_f d\tilde{t} \quad (3e)$$

$\tilde{r}$  is the radius,  $\tilde{m}$  the mass flow rate,  $\tilde{u}$  the gas velocity,  $\tilde{U}_f$  the moving velocity of the flamefront,  $\tilde{Y}_F$  and  $\tilde{Y}_O$  the mass fractions of fuel and oxygen, respectively,  $\tilde{T}$  the temperature,  $\tilde{Q}$  the heat release rate per unit mass of fuel,  $\tilde{\rho}$  the density,  $\tilde{\omega}$  the reaction rate, and  $\nu_O$  and  $W_O$  the molar stoichiometric coefficient ratio and the molecular weight ratio of oxygen to fuel, respectively.

The boundary conditions in the far field from the droplet are

$$\begin{aligned} \tilde{r} \rightarrow \infty: \quad \tilde{T} &= \tilde{T}_\infty, \quad \tilde{Y}_F = 0, \\ \tilde{Y}_O &= \tilde{Y}_{O,\infty}, \quad \tilde{u} = 0 \end{aligned} \quad (4a)$$

while those at the droplet surface are

Mass conservation

$$\tilde{\rho}_l \frac{d\tilde{r}_s}{d\tilde{t}} = -\tilde{\rho}_s \tilde{u}_s \left( 1 - \frac{1}{\tilde{u}_s} \frac{d\tilde{r}_s}{d\tilde{t}} \right) \quad (4b)$$

$$\begin{aligned} \tilde{m}_s &= \tilde{r}_s^2 \tilde{\rho}_s (\tilde{u}_s - \tilde{U}_f) = \\ &- \tilde{r}_s^2 \tilde{\rho}_l \frac{d\tilde{r}_s}{d\tilde{t}} \left( 1 - \frac{\tilde{\rho}_s}{\tilde{\rho}_l} + \frac{\tilde{\rho}_s}{\tilde{\rho}_l} \frac{\tilde{U}_f}{d\tilde{r}_s/d\tilde{t}} \right) \end{aligned} \quad (4c)$$

Fuel conservation

$$\begin{aligned} \tilde{\rho}_s (1 - Y_{f,s}) \left( \tilde{u}_s - \frac{d\tilde{r}_s}{d\tilde{t}} \right) \\ + (\tilde{\rho}\tilde{D}) \left. \frac{\partial Y_{F,s}}{\partial \tilde{r}} \right|_s = 0 \end{aligned} \quad (4d)$$

Energy conservation

$$\begin{aligned} \tilde{\lambda} \left. \frac{\partial \tilde{T}}{\partial \tilde{r}} \right|_s - \tilde{\rho}_s \left( \tilde{u}_s - \frac{d\tilde{r}_s}{d\tilde{t}} \right) \frac{\tilde{L}}{\tilde{c}_p} \\ + \frac{1}{3} \frac{\tilde{c}_{pl}}{\tilde{c}_p} \frac{d\tilde{T}_s}{d\tilde{t}} = 0 \end{aligned} \quad (4e)$$

where  $\tilde{L}$  is the latent heat of vaporization. For a general description of the problem, the Clausius-Clapeyron equation is needed to determine the mass fraction of fuel in the gas phase at the droplet surface; however, it is not essential for the present study, and we close the formulation by assuming that the surface temperature of the droplet is a constant,  $\tilde{T}_s$ .

### Quasi-Steady Approximation with Consideration of Flamefront Motion

As discussed earlier, a very small moving velocity of the flamefront can induce a significant modification of the mass flow rate. In the present analysis, we consider situations for which  $\kappa_{CQS} = O(\varepsilon^{-1/3}) \gg 1$  with  $\varepsilon \ll 1$ , and with the moving velocity of the flamefront having a magnitude

$$U_f \equiv \frac{dr_f}{dt} = \frac{\tilde{U}_f}{\tilde{u}_s} = \kappa_{CQS} \varepsilon = O(\varepsilon^{2/3}) \ll 1 \quad (5)$$

The difference in the mass flow rate between the droplet surface and the flamefront is

$$\begin{aligned} (\tilde{m}_f/\tilde{m}_s - 1) &\approx \frac{\tilde{\rho}_f \tilde{r}_f^2 (\tilde{u}_f - \tilde{U}_f)}{\tilde{\rho}_s \tilde{r}_s^2 \tilde{u}_s} - 1 \\ &\approx - \left( \frac{\tilde{\rho}_f}{\tilde{\rho}_s} \cdot \frac{\tilde{r}_f^2}{\tilde{r}_s^2} \cdot \frac{\tilde{U}_f}{\tilde{u}_s} \right) = O(1) \end{aligned} \quad (6)$$

for  $O(1)$  density ratio  $\tilde{\rho}_f/\tilde{\rho}_s$ . The nonlinear coupling, appearing in equation 3, indicates that general solutions to the unsteady droplet combustion problems are difficult to obtain. However, we do not expect the unsteady effect (in the flame coordinate) to

change the qualitative features. Thus by neglecting the unsteady terms appearing in equations 3, 4, the equations are simplified to the following quasi-steady system in the flame coordinate,

$$\begin{aligned} \frac{\partial m}{\partial \xi} - \frac{2U_f}{Pe} r^3 \rho &= 0, & m \frac{\partial S_T}{\partial \xi} &= -\frac{\partial^2 S_T}{\partial \xi^2} \\ m \frac{\partial S_F}{\partial \xi} &= -\frac{\partial^2 S_F}{\partial \xi^2} \end{aligned} \tag{7}$$

where we have introduced

$$d\xi = -Pe \frac{1}{r^2} dx, \quad Pe \equiv \frac{\tilde{m}_s}{\tilde{\rho} \tilde{D} \tilde{r}_s} \tag{8a}$$

$$m = \frac{\tilde{m}}{\tilde{m}_s}, \quad u = \frac{\tilde{u}}{\tilde{u}_s}, \quad r = \frac{\tilde{r}}{\tilde{r}_s}$$

$$x = \frac{\tilde{x}}{\tilde{r}_s}, \quad dt = \frac{\tilde{u}_s d\tilde{t}}{\tilde{r}_s} \tag{8b}$$

$$\rho = \frac{\tilde{\rho}}{\tilde{\rho}_s} = \frac{\tilde{T}}{\tilde{T}_s}, \quad Q = \frac{\tilde{Q}}{\tilde{c}_p \tilde{T}_s}, \quad L = \frac{\tilde{L}}{\tilde{c}_p \tilde{T}_s}$$

$$T = \frac{\tilde{c}_p \tilde{T}}{\tilde{Q}}, \quad \alpha_O = \frac{\tilde{Y}_O}{v_O W_O}, \quad \alpha_F = \tilde{Y}_F \tag{8c}$$

and

$$S_T = T + \alpha_O, \quad S_F = \alpha_F - \alpha_O \tag{9}$$

The boundary conditions are

$$\begin{aligned} r \rightarrow \infty: \xi &= 0, & S_{T,\infty} &= T_\infty + \alpha_{O,\infty} \\ S_{F,\infty} &= -\alpha_{O,\infty} \end{aligned} \tag{10}$$

and

$$r = r_s : \xi = \xi_s, \quad S_{T,s} = T_s \tag{11}$$

$$\frac{dS_{T,s}}{d\xi} = -H, \quad \frac{dS_{F,s}}{d\xi} = 1 - S_{F,s} \tag{12}$$

where  $H = L/Q$  and  $Pe$  is the Péclet number. The problem is now similar to that in Ref. [4], in which the influence of the droplet surface regression rate is considered.

After integrating these equations using the boundary conditions, we obtain the gradients for  $S_T$  and  $S_F$

$$\begin{aligned} \frac{dS_T}{d\xi} &= -H \exp\left(-\int_{\xi_s}^{\xi} md\xi\right) \\ \frac{dS_F}{d\xi} &= (1 - \alpha_{F,s}) \exp\left(-\int_{\xi_s}^{\xi} md\xi\right) \end{aligned} \tag{13}$$

and the spatial distribution for  $m$ ,  $S_T$ , and  $S_F$

$$\begin{aligned} m &= 1 + \frac{2U_f}{Pe} f(\xi, Pe), \quad f(\xi, Pe) \equiv \int_{\xi_s}^{\xi} \rho r^3 d\xi \\ \xi &= Pe \frac{1}{r}, \quad \xi_s = Pe \end{aligned} \tag{14a}$$

$$\begin{aligned} S_T &= (T_\infty + \alpha_{O,\infty}) - HI(\xi, U_f, Pe) \\ S_F &= -\alpha_{O,\infty} + (1 - \alpha_{F,s})I(\xi, U_f, Pe) \end{aligned} \tag{14b}$$

with

$$I(\xi, U_f, Pe) \equiv \int_0^{\xi} \left[ \exp\left(-\int_{\xi_s}^{\xi} md\xi\right) \right] d\xi \tag{14c}$$

where the fuel concentration at the droplet surface is the same as that of the CQS approximation case,

$$\begin{aligned} Y_{F,s} &= 1 - \frac{1 + \alpha_{O,\infty}}{1 + B} \\ \text{with } B &\equiv \frac{T_\infty - T_s + \alpha_{O,\infty}}{H} \end{aligned} \tag{15}$$

For a given position of the flamefront,  $Pe$  and  $U_f$  can be determined from the following two integral equations,

$$I_s(\xi_s, U_f, Pe) - B = 0 \tag{16a}$$

$$I_f(\xi_f, U_f, Pe) - \frac{\alpha_{O,\infty}}{1 - \alpha_{F,s}} = 0 \tag{16b}$$

Equations 16a and 16b can only be integrated numerically. However, before presenting the numerical results, let us first analyze their properties.

When the flamefront is motionless,  $U_f = 0$ , equations 16a and 16b simplifies to the CQS approximation,

$$S_T = (T_\infty + \alpha_{O,\infty}) + H(1 + B)[\exp(-\xi) - 1] \tag{17}$$

$$S_F = -\alpha_{O,\infty} - (1 + \alpha_{O,\infty})[\exp(-\xi) - 1] \tag{18}$$

$$Pe = \xi_s = \ln(1 + B), \quad \xi_f = \ln(1 + \alpha_{O,\infty}) \tag{19}$$

$$r_f/r_s = \ln(1 + B)/\ln(1 + \alpha_{O,\infty}) = \kappa_{CQS} \tag{20}$$

As noted in the Introduction, equation 20 gives a moving velocity,  $U_f \equiv dr_f/dt = \kappa_{CQS}\varepsilon$ . When  $\kappa_{CQS} = O(1)$ , the effect of the motion of the flamefront is of the order of  $\varepsilon$  and can be neglected. When  $\kappa_{CQS} = O(\varepsilon^{-1/3})$ , the CQS approximation is no longer self-consistent, and the effect of the motion of the flamefront must be taken into account.

Equations 16a and 16b determine  $Pe$  and  $U_f$  in terms  $r_f$ . For an evolution problem, the flamefront position and its velocity are related via equation 5. In this manner, for a given initial reaction front position and droplet size, we can completely determine the trajectory of both the reaction front and the droplet surface.

The existence of solutions for equations 16a and

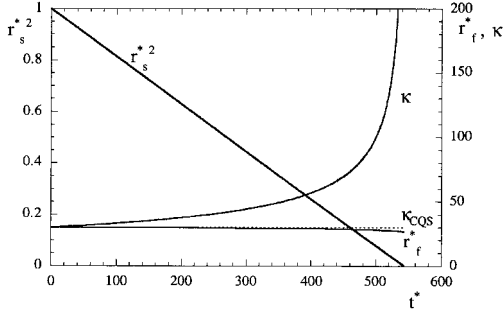


FIG. 1. Temporal variation of the square of the droplet radius, standoff ratio, and flamefront position for a heptane droplet ( $\kappa_{\text{CQS}} = 30$ ,  $Q_s = 27$ ) burning in the standard atmosphere. The initial condition corresponds to the classical quasi-steady solution (CQS).  $r_b = 2500$  for this case. The nondimensional droplet radius, flamefront position, and time are defined as  $r_s^* = \tilde{r}_s/\tilde{r}_{s,0}$ ,  $r_f^* = \tilde{r}_f/\tilde{r}_{s,0}$ ,  $t^* = \tilde{t}/(\tilde{r}_{s,0}/\tilde{U}_{s,0})$ .

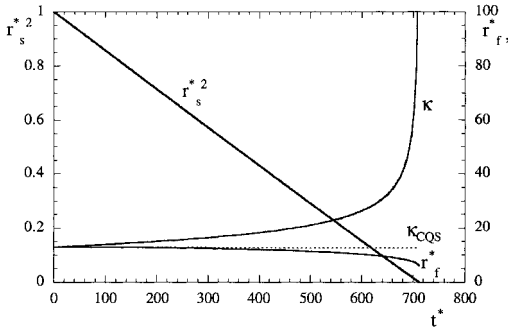


FIG. 2. Temporal variation of the square of the droplet radius, standoff ratio, and reaction front position for an ethanol droplet ( $\kappa_{\text{CQS}} = 13$ ,  $Q_s = 2$ ) burning in the standard atmosphere. The initial condition corresponds to the classical quasi-steady solution (CQS).

16b, with boundary conditions given in equations 10–12, should be discussed. For this purpose, we only need to know the behavior of  $I(\xi)$ , given in equation 14c, in the far field. In distances very far from the droplet surface, the density variation is small and can be neglected. After integrating equation 14c with constant density, we find that  $I$  takes the form

$$I(r, Pe) \sim \int \frac{1}{r^2} \exp\left(-\frac{1}{r} - \frac{2U_f}{Pe} r\right) dr \quad (21)$$

For an outwardly spreading front with  $U_f > 0$ , the integral is convergent, and we can expect the existence of solutions for equations 16a and 16b. For an inwardly spreading reaction front with  $U_f < 0$ ,  $I$  diverges, implying that solutions satisfying the boundary conditions given in equation (10) do not exist.

This singularity problem in the cold boundary has been previously pointed out by Williams [4]. The mathematical difficulty arises because, in the far field, equation 7 is simplified to diffusion equations with negative coefficients. Physically, this means that the unsteady effect in the far field is important and has to be considered in order to eliminate the singularity.

We are interested in the range of  $U_f$  of the order of  $\kappa_{\text{CQS}}\varepsilon$ . The integral, equation 21, converges for  $r$  as large as  $(\kappa_{\text{CQS}}\varepsilon)^{-1} \gg 1$ . Therefore, solutions with  $U_f < 0$  exist when computationally we replace the boundary location  $r \rightarrow \infty$  in equation 10 by a finite value  $r_b$ . When the far-field unsteady effect is considered, the largest contribution to the integral comes from the region near the reaction front. Thus it is reasonable to expect that changing the far-field boundary location would not affect the results very much.

## Results

As mentioned earlier, the critical parameter governing the global validity of the CQS theory is the ratio of the fuel mass in the gas-phase region to that of the droplet, namely  $Q_s \equiv \varepsilon\kappa_{\text{CQS}}^3 \ll 1$ . With  $\varepsilon$  being much smaller than unity in subcritical conditions for hydrocarbon fuels, we examine the flame behavior as a function of the magnitude of  $\kappa_{\text{CQS}}$ . The physical cases to be presented are *n*-heptane burning in air ( $\kappa_{\text{CQS}} = 30$ ,  $Q_s \approx 27$ ), ethanol burning in air ( $\kappa_{\text{CQS}} = 13$ ,  $Q_s \approx 2$ ), and ethanol burning in pure oxygen ( $\kappa_{\text{CQS}} = 6.7$ ,  $Q_s \approx 0.3$ ). An artificial case of  $\kappa_{\text{CQS}} = 4$  ( $Q_s \approx 0.07$ ) is also presented to represent situations of very small  $Q_s$ . The property values used in the calculations are those given in Ref. [9]. We also examine the flame behavior due to the initial condition, that is, when the flame position initially corresponds to the CQS solution and when it is initially displaced from CQS. In all calculations,  $r_b = 1500$  is used for the boundary location of equation 10. We have also used  $r_b = 2500$ , with no significant differences noticeable.

Figures 1 through 4 represent cases in which the flame is initially located at the position determined by CQS theory, with  $U_f = 0$  at  $t = 0$ , for the first four cases mentioned earlier. It is seen that as the droplet evaporates and its surface regresses, the flamefront spreads inwardly ( $U_f < 0$ ). For the cases when the standoff ratio is large, as for *n*-heptane and ethanol burning in air (Figs. 1 and 2),  $\kappa$  increases with time and tends to infinity as the droplet size goes to zero. With  $Q_s > 2$ , the flame response cannot be maintained by the CQS solution. Physically, this is because the volume of fuel vapor is so large—in fact there is more fuel mass in the gas phase than in the liquid phase of the droplet—that the flame practically does not respond to changes in droplet size.

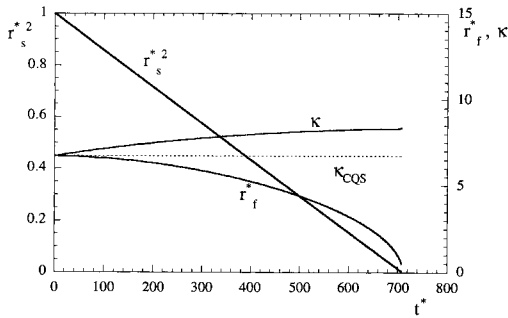


FIG. 3. Temporal variation of the square of the droplet radius, standoff ratio, and reaction front position for an ethanol droplet ( $\kappa_{\text{CQS}} = 6.7$ ,  $Q_s = 0.3$ ) burning in pure oxygen. The initial condition corresponds to the classical quasi-steady solution (CQS).

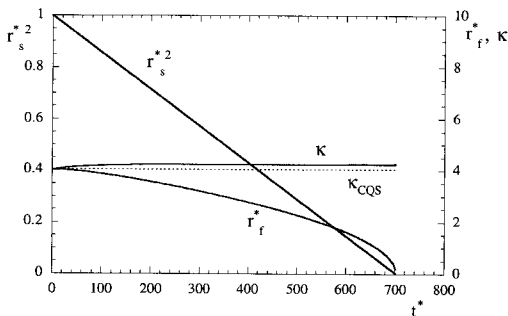


FIG. 4. Temporal variation of the square of the droplet radius, standoff ratio, and reaction front position for a theoretical droplet ( $\kappa_{\text{CQS}} = 4$ ,  $Q_s = 0.07$ ) burning in pure oxygen. The initial condition corresponds to the classical quasi-steady solution (CQS).

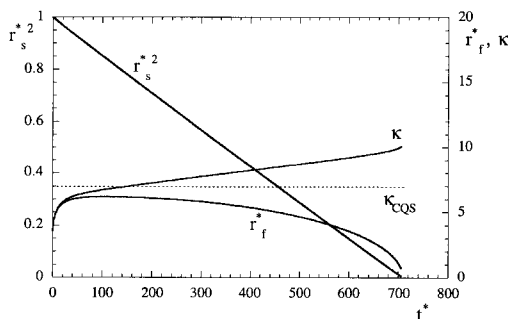


FIG. 5. Temporal variation of the square of the droplet radius, standoff ratio, and reaction front position for an ethanol droplet ( $\kappa_{\text{CQS}} = 6.7$ ,  $Q_s = 0.3$ ) burning in pure oxygen. The droplet is ignited at a radius smaller than the classical quasi-steady solution (CQS).  $r_b = 2500$  for this case.

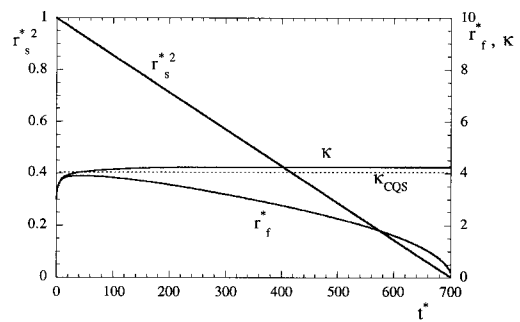


FIG. 6. Temporal variation of the square of the droplet radius, standoff ratio, and reaction front position for a theoretical droplet ( $\kappa_{\text{CQS}} = 4$ ,  $Q_s = 0.07$ ) burning in pure oxygen. The droplet is ignited at a radius smaller than the the classical quasi-steady solution (CQS).

Thus, with a large flame standoff ratio, the mass of fuel consumed by a relatively small displacement in the flame location is of the order of the mass of the droplet. This explains the small change in the flame position  $r_f^* \equiv \tilde{r}_f/\tilde{r}_{s,0}$  of Figs. 1 and 2 during the entire droplet lifetime. For ethanol burning in pure oxygen (Fig. 3),  $Q_s \sim 0.3 < 1$ . Thus, while  $\kappa$  still increases with time, it does not tend to infinity. Instead it approaches a finite value as the droplet size goes to zero. For this case, since there is more fuel mass in the droplet than in the vapor outside it, the flame ( $r_f^*$  of Fig. 3) can respond to the regressing droplet. Consequently,  $\kappa$  is close to the CQS solution, but slightly exceeding it as previously shown in Ref. [6]. Finally, for our theoretical fuel (Fig. 4), which possesses a small standoff ratio with  $Q_s \sim 0.07$ , we find that the CQS solution is a satisfactory approximation. The flame position is largely dictated by the instantaneous mass flow rate of the fuel vapor from the surface of the droplet. Finally, we see that for all cases presented in Figs. 1 through 4, the approximate linearity of  $\tilde{r}_s^2 - v_s - \tilde{t}$  is very well kept.

We next incorporate effects of the initial flame displacement from the CQS position. Figs. 5 and 6 represent the same cases as Figs. 3 and 4, respectively, but with the flame initially located at  $r_f^* < r_{f,\text{CQS}}^*$ , due to ignition at a position closer to the droplet surface. For these two cases, the flamefront initially spreads outwardly ( $U_f > 0$ ) because the evaporation rate at the droplet surface is larger than the consumption rate at the flamefront, resulting in an accumulation of the fuel vapor between the droplet surface and the flame [6]. As  $\kappa$  moves towards the CQS position, it is obvious from Figs. 5 and 6 that the time scale for this quasi-steady accumulation effect decreases dramatically with decreasing  $\kappa_{\text{CQS}}$ . With a naturally smaller standoff ratio, the amount of fuel vapor needed to be built up to approach the fuel concentration profiles of CQS state is considerably less. As shown in Fig. 6, for the theoretical

fuel ( $Q_s \sim 0.07$ ), the flame reaches the steady state close to the CQS state within a time scale much shorter than the droplet lifetime. Therefore, similar to the arguments for the previously discussed depletion effect, the quasi-steady mass accumulation effect is important and constitutes a significant portion of the droplet lifetime when  $Q_s = O(1)$  and can be neglected when  $Q_s \ll 1$ .

As can be seen from the preceding results, the qualitative effect of the flamefront motion primarily depends only on  $Q_s$ . For the cases where the flame standoff distance is initially closer to the droplet than predicted by the CQS theory, the physical flame size  $r_f^*$  initially increases and then decreases (Figs. 5 and 6), as predicted by the transient theories. Nevertheless, regardless of how  $\kappa$  responds, the results evince that the  $d^2$ -law is adequate in predicting the vaporization rate and the instantaneous droplet size. As discussed in many previous works [7–10], even though significant changes continuously occur in regions far away from the droplet, the droplet evaporation rate is primarily controlled by processes in its vicinity. We have examined the vapor and temperature profiles predicted by the present theory for *n*-heptane and have found that the temperature/mass fluxes at the droplet surface are fairly constant in time, notwithstanding changes far away. Apart from the initial transient,  $Pe$  at the droplet surface remains fairly constant, and the magnitude of  $U_f$  is on the order of  $\kappa\varepsilon$ , consistent with our analysis.

### Concluding Remarks

The new criterion given in equations 1a and 1b allows us to address the long-standing question of the validity of the application of the  $d^2$ -law to describe the droplet combustion process, especially the empirically observed flame-front motion. When the quasi-steady parameter  $Q_s$  is much smaller than unity, the  $d^2$ -law is a good approximation to describe the flame position, and the effect of fuel vapor accumulation or depletion is relatively weak. However, for  $Q_s = O(1)$ , the motion of the reaction front constitutes a crucial factor in the problem, directly affecting the stand-off ratio and producing a significant difference of that value with the CQS theory. In such a case, the adoption of the  $d^2$ -law leads to incorrect estimates on the heat release rate during droplet and spray combustion. Our quasi-steady solution incorporating the motion of the reaction front confirms the criterion given in equations 1a and 1b. Furthermore, all present results related to effects of fuel vapor accumulation are consistent with those previously predicted by a phenomenologically motivated formulation and observed experimentally on the movement of the flamefront for large and small flame sizes [6].

The present criterion also explains the seemingly

contrasting results of Marchese et al. [14], which suggest that the CQS solution attracts the unsteady solution from ignition and that the mass accumulation effect is weak for their microgravity experiments with methanol/water droplets, as compared with those of King [15], which show that quasi-steady conditions are not reached during the entire lifetime of *n*-heptane droplets burning in air. The difference is due to the small flame sizes ( $\kappa_{CQS} \sim 4$ ) of Ref. [14], versus the substantially larger flame sizes ( $\kappa_{CQS} \sim 30$ ) of Ref. [15], due to the unity Lewis number assumption. Finally, the unsteady numerical calculations of Ref. [14], for  $\kappa_{CQS} \sim 4$ , has produced results that are very similar to those of the CQS theory, indicating that far-field unsteady diffusion effects treated in Refs. [9] and [10] are not the primary source for the flame unsteadiness. Thus it appears that for subcritical burning, the role of far-field unsteady diffusion is primarily mathematical in nature in that it eliminates the cold boundary singularity imposed by the quasi-steady assumption.

### Acknowledgments

This research was jointly supported by the NASA Microgravity Combustion Program under the technical management of Dr. K. Sacksteder, and by the Air Force Office of Scientific Research under the technical management of Dr. M. Birkan.

### REFERENCES

1. Godsave, G. A. E., in *Fourth Symposium (International) on Combustion*, The Combustion Institute, Pittsburgh, 1953, pp. 818–830.
2. Spalding, D. B., in *Fourth Symposium (International) on Combustion*, The Combustion Institute, Pittsburgh, 1953, pp. 847–864.
3. Goldsmith, M. and Penner, S. S., *Jet Propulsion*, 24:245–251 (1954).
4. Williams, F. A., *J. Chem. Phys.* 33:133–144 (1960).
5. Kumagai, S., Sakai, T., and Okajima, S., in *Thirteenth Symposium (International) on Combustion*, The Combustion Institute, Pittsburgh, 1971, pp. 778–785.
6. Law, C. K., Chung, S. H., and Srinivasan, N., *Combust. Flame* 38:173–198 (1980).
7. Law, C. K., *Prog. Energy Combust. Sci.* 8:169–199 (1982).
8. Williams, F. A., *Combustion Theory*, 2<sup>nd</sup> ed., Benjamin/Cummings, Menlo Park, CA, 1985.
9. Waldman, C. H., in *Fifteenth Symposium (International) on Combustion*, The Combustion Institute, Pittsburgh, 1975, pp. 429–442.
10. Crespo, A. and Liñán, A., *Combust. Sci. Technol.* 11:9–18 (1975).
11. Botros, P., Law, C. K., and Sirignano, W. A., *Combust. Sci. Technol.* 21:123–130 (1980).

12. Rosner, D. E. and Chang, W. S., *Combust. Sci. Technol.* 7:145–158 (1973).
13. Williams, F. A., *Acta Astronautica* 12:547–553 (1985).
14. Marchese, A. J., Dryer, F. L., Colantonio, R. O., and Nayagam, V., in *Twenty-Sixth Symposium (International) on Combustion*, The Combustion Institute, Pittsburgh, 1996, pp. 1209–1217.
15. King, M. K., in *Twenty-Sixth Symposium (International) on Combustion*, The Combustion Institute, Pittsburgh, 1996, pp. 1227–1234.

## COMMENTS

*Jerry M. Seitzman, Georgia Institute of Technology, USA.* Regarding droplet lifetime, how do your results quantitatively differ from those of the quasi-steady-state model?

*Author's Reply.* The droplet surface regression rate is not affected much from the  $d^2$ -law value, as is usually the case for droplet burning in the absence of intense droplet heating. However, because the rate of fuel gasification at the droplet surface is not the same as the rate of fuel consumption at the flame front, due to flame-front motion with associated fuel vapor accumulation/depletion, the heat-release rate can be significantly modified. Thus, in direct response to your question, the droplet lifetime is close to that predicted by the  $d^2$ -law; however, the actual combustion time may be significantly different.

•

*F. A. Williams, University of California–San Diego, USA.* I believe that your analysis has special relevance to the final stage of droplet combustion. Purely computational approaches have difficulty in describing the burn out of the small fuel vapor cloud that remains after the droplet disappears. Your considerations could help to clarify this.

*Author's Reply.* We believe our analysis is of relevance to the entire period of droplet burning, simply because we have enforced strict mass conservation by explicitly considering the motion of the flame front. As a result, the present work has shown that when the stand-off ratio is large enough, a fuel vapor pocket remains after the disappearance of the droplet. As you have pointed out, it is worth extending our analysis to this regime so that the phenomenon at this final stage of droplet combustion can be better understood.